한국측량학회지, 제 25권 제 6-1호, pp. 575~583(2007년 12월 31일)

A Region Based Approach to Surface Segmentation using LIDAR Data and Images

Jiyoung Moon[1] · Impyeong Lee[2]

Abstract

Surface segmentation aims to represent the terrain as a set of bounded and analytically defined surface patches. Many previous segmentation methods have been developed to extract planar patches from LIDAR data for building extraction. However, most of them were not fully satisfactory for more general applications in terms of the degree of automation and the quality of the segmentation results. This is mainly caused from the limited information derived from LIDAR data. The purpose of this study is thus to develop an automatic method to perform surface segmentation by combining not only LIDAR data but also images. A region-based method is proposed to generate a set of planar patches by grouping LIDAR points. The grouping criteria are based on both the coordinates of the points and the corresponding intensity values computed from the images. This method has been applied to urban data and the segmentation results are compared with the reference data acquired by manual segmentation. 76% of the test area is correctly segmented. Under-segmentation is rarely founded but over-segmentation still exists. If the over-segmentation is mitigated by merging adjacent patches with similar properties as a post-process, the proposed segmentation method can be effectively utilized for a reliable intermediate process toward automatic extraction of 3D model of the real world.

Keywords : LIDAR, Image, Segmentation, Data fusion, Region growing

1. Introduction

Surface segmentation is a process to represent the terrain as a set of bounded and analytically defined surface patches by extracting these patches from sensory data. It has been recognized as an important intermediate process toward the automatic generation of abstract descriptions of the real world from sensory data (Lee, 2002; Lee and Schenk 2001b; Lee and Schenk 2002; Lee, 2006a). Recently, with the advance of sensor technology, LIDAR systems that can generate a number of points densely sampled from the surface of the earth have emerged as a promising means to capture 3D information efficiently and accurately.

Surface segmentation from such LIDAR data has been attempted by many researchers. Most of them performed segmentation as an intermediate process for the extraction of artificial objects such as buildings or roads. For building reconstruction, Brenner (2003) proposed a RANSAC based estimation method to extract planar patches from a DSM generated from LIDAR data. Rottensteiner (2003) considered the normal vector at each grid post on the DSM to extract planar patches. Lodha et. al. (2005) presented a semi-automatic method to segment planar patches using K-mean algorithm for roof reconstruction. For more general purposes, Lee and Schenk (2001a) and Lee (2006a) have proposed an automatic method to generate a set of planar patches from LIDAR points by grouping them using a region-growing approach. Lee (2006b) has applied this approach to extracting ground points and Park et. al. (2006) and Kim (2006) have used for extracting 3D models of buildings and roads, respectively.

The automatic segmentation results from LIDAR data

1) National Geographic Information Institute, 111 Wonchon-dong, Yeongtong-Gu, Suwon-Shi, Kyonggi-Do, Korea (E-mail: jymoon@moct.go.kr)
2) Corresponding author, Dept. of Geoinformatics, The University of Seoul, 90 Jeonnong-dong, Dongdaemun-gu, Seoul, Korea (E-mail: iplee@uos.ac.kr)

using the previously proposed algorithms are not fully satisfied due to various reasons. For examples, many algorithms suffered from the under-segmentation problems that tend to undesirably merge more than two separate patches in reality into a patch. One of the most important reasons to produce the unsatisfied results is that most methods consider only the coordinates of the LIDAR points. Some LIDAR systems also provide the intensity value of each point proportional to the energy of reflected pulse but the quality is not sufficient for segmentation. In other hand, aerial images have many complementary characteristics to the LIDAR data (Schenk and Csatho, 2002). For example, LIDAR data have only the geometric information such as the coordinates of the sampled points but the images also include radiometric information such as the intensity values for each band. In this study, we thus attempted to develop an automatic segmentation approach using both LIDAR data and aerial images. Since both data are complementary to each other, more appropriate segmentation results are expected.

In general, segmentation methods are classified into edge-based or region-based approach. An edge based approach extracts the discontinuous edges like road boundaries or building outlines and attempts to link the edges into a closing region. However, this linking process may often fail since some of the edges encompassing a region are often missing or quite scattered. A region based approach generates a region by starting from a small homogeneous region called *seed region* and iteratively adding a new sensory element adjacent to the currently growing region. The sensory element can be a point of LIDAR data or a pixel of an image. During the growing process, the new element is examined using an *inclusion test* to determine whether it is enough consistent with the growing region. For more successful results from the region based approach, the approach is required to employ more sophisticated strategy for seed region selection and inclusion test.

The proposed method of this study is classified as a region-based method. Seed patches are generated by clustering a small number of points adjacent to each other and then selected in the order of their homogeneity in terms of geometry and intensity. Starting from a selected seed patch, it grows a large patch by recursively adding a new point adjacent to and consistent with the patch. The consistency is examined using a novel statistical test to determine statistically whether it is significantly evident that the new point has the same properties as the patch in terms of geometry and intensity.

After this introduction, this paper describes in detail the methodology focusing on seed patch selection and iterative growing process. The experiment results from its application to urban data are then presented with some quantitative analysis, followed by some concluding remarks.

2. Methodology

The proposed segmentation approach consists of two stages. In the first stage, we generate a number of seed patch candidates, some of which are selected for patch growing in the second stage. In addition, it is assumed that the LIDAR data have been preprocessed using the outlier elimination (Moon et. al., 2005) and calibration techniques and the images have been geometrically registered with the preprocessed LIDAR data (Lee et. al., 2005). After this geometric registration, the exterior orientation parameters of the images are then determined with respect to the same reference coordinate system as the LIDAR data. With these exterior orientation parameters, each LIDAR point can be projected to the image based on the collinearity equation. The intensity values interpolated at this projected location on the image can be assigned to the corresponding intensity to the LIDAR point.

2.1 Seed patch generation

Seed patches serve as the initial patches from which surface patches start to grow in the next stage. In this study, we generate a set of seed patches by clustering a certain number of points close to each point of LIDAR data. The properties of each seed patch indicating its geometry and intensity are then computed. In terms of the geometry, the plane parameters of each patch are estimated by fitting a planar model to a set of the points clustered to the patch. If a seed patch includes k points, the observation equations to estimate the plane parameters (a, b, c) are represented as

$$y_I = A_I \xi_I + e_I, \quad e_I \sim (0, \sigma_I^2 I_k), \tag{1}$$

$$y_I \equiv \begin{bmatrix} z_1 \\ z_2 \\ \vdots \\ z_k \end{bmatrix}, A_I \equiv \begin{bmatrix} x_1 & y_1 & 1 \\ x_2 & y_2 & 1 \\ \vdots & \vdots & \vdots \\ x_k & y_k & 1 \end{bmatrix}, \xi_I \equiv \begin{bmatrix} a \\ b \\ c \end{bmatrix}, e_I \equiv \begin{bmatrix} e_1 \\ e_2 \\ \vdots \\ e_k \end{bmatrix}, \tag{2}$$

where (x_i, y_i, z_i) are the coordinates of i-th point of the patch, e_i is the combined error associated with the coordinates, and I_k is the k by k identity matrix. In terms of intensity, the mean values (R, G, B) of the intensity of image pixels corresponding to the points of the patch are estimated using the observation equations expressed as

$$y_{II} = A_{II} \xi_{II} + e_{II}, \quad e_{II} \sim (0, \sigma_{II}^2 I_{3k}), \tag{3}$$

$$y_{II} \equiv \begin{bmatrix} R_1 \\ G_1 \\ B_1 \\ \vdots \\ R_k \\ G_k \\ B_k \end{bmatrix}, A_{II} \equiv \begin{bmatrix} 1 & 0 & 0 \\ 0 & 1 & 0 \\ 0 & 0 & 1 \\ \vdots & \vdots & \vdots \\ 1 & 0 & 0 \\ 0 & 1 & 0 \\ 0 & 0 & 1 \end{bmatrix}, \xi_{II} \equiv \begin{bmatrix} R \\ G \\ B \end{bmatrix}, e_{II} \equiv \begin{bmatrix} e_{R1} \\ e_{G1} \\ e_{B1} \\ \vdots \\ e_{Rk} \\ e_{Gk} \\ e_{Bk} \end{bmatrix}, \tag{4}$$

where (R_i, G_i, B_i) are the intensity values corresponding to the i-th point when the image has three bands.

By applying the least squares estimation method to the two sets of the observation equations in Eq. (1) and (3), the estimates for the parameters and the variance components can be derived as

$$\hat{\xi}_I = (A_I^T A_I)^{-1} A_I^T y_I, \tag{5}$$

$$\hat{\xi}_{II} = (A_{II}^T A_{II})^{-1} A_{II}^T y_{II}, \tag{6}$$

$$\hat{\sigma}_I^2 = \frac{y_I^T y_I - y_I^T A_I \hat{\xi}_I}{k-3}, \tag{7}$$

$$\hat{\sigma}_{II}^2 = \frac{y_{II}^T y_{II} - y_{II}^T A_{II} \hat{\xi}_{II}}{3k-3}. \tag{8}$$

The estimate $\hat{\xi}_{II}$ derived in Eq. (6) is actually identical to the average intensity values corresponding to all the points of the patch. The square root of the variance component estimate derived in Eq. (7) is roughly proportional to the average distance between each point and the plane adjusted to the set of points of the patch, actually indicating the *roughness* of the patch. The square root of the variance component estimate derived in Eq. (8) is roughly proportional to the standard deviation of the intensity values corresponding to the points of the patch. Hence, both variance component estimates indicate the homogeneity of the patch in terms of the geometry and intensity, respectively.

2.2 Iterative growing

This process generates a set of surface patches by growing from some of the seed patches generated in the previous stages. It starts with the selection of a seed patch among a number of seed patch candidates generated in the previous stage. Among these candidates, a seed patch of higher homogeneity in terms of geometry and intensity has higher priority to be selected. The geometric homogeneity is quantified with the plane fitting errors, so called roughness and the intensity homogeneity is done with the variation of the intensity values assigned to each point of a seed patch. These two kinds of homogeneity measures have been derived in Eq. (7) and (8), respectively. If the most homogeneous one has been already segmented as a part of previously growing patch, we will discard it and use the next most homogeneous one. This selection process is similar to those process employed by Lee (2006) to extract planar patches from only LIDAR data except the consideration of the intensity homogeneity.

From the seed patch of the highest priority, we generate a surface patch using the iterative growing process. This process iteratively adds a point into the currently growing patch if the point is adjacent to and consistent with the patch. The overview of this process is summarized in Fig. 1.

The most important step of this iterative growing process is the inclusion test to determine whether a new point is included to a patch or not by checking its consistency with the patch in terms of geometry and intensity. In terms of geometry, we statistically determine if the point can be thought be on the plane of the patch. At the same time, in terms of intensity, we statistically determine if the image value assigned to the point can be thought be the same of the mean intensity values assigned to the points of the patch.

This test is configured with a statistical test in which

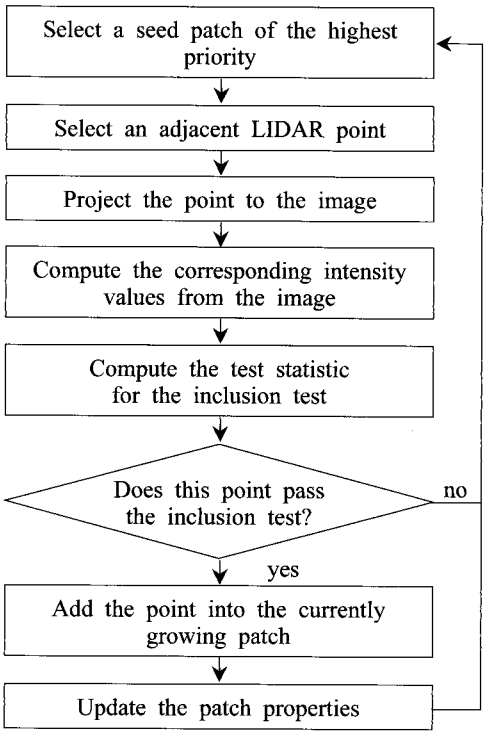

Fig. 1. Iterative growing process

a hypothesis is established and examined with F-test. In this test, the null hypothesis (H_0) is "the new point has the same properties as the currently growing patch" and the alternative hypothesis (H_1) is "the new point does not have the same properties as the currently growing patch". These hypotheses are mathematically represented as

$$H_0 : y_{n+1} = A_{n+1}\hat{\xi}_{(n)} \quad \text{vs.} \quad H_1 : y_{n+1} \neq A_{n+1}\hat{\xi}_{(n)}, \tag{9}$$

where $\hat{\xi}_{(n)}$ is the estimate of the parameters of the current patch that have already included n number of points. This estimate is based on the observation equations incorporating Eq. (1) and Eq. (3) expressed as

$$y_{(n)} = A_{(n)}\xi_{(n)} + e_{(n)}, \quad e_{(n)} \sim (0, \sigma_0^2 Q), \tag{10}$$

$$y_{(n)} \equiv \begin{bmatrix} y_{I(n)} \\ y_{II(n)} \end{bmatrix}, A_{(n)} \equiv \begin{bmatrix} A_{I(n)} & 0 \\ 0 & A_{II(n)} \end{bmatrix}, \xi_{(n)} \equiv \begin{bmatrix} \xi_{I(n)} \\ \xi_{II(n)} \end{bmatrix},$$
$$e_{(n)} \equiv \begin{bmatrix} e_{I(n)} \\ e_{II(n)} \end{bmatrix}, Q \equiv \begin{bmatrix} I_k & 0 \\ 0 & \sigma_{II}^2/\sigma_0^2 I_{3k} \end{bmatrix} \tag{11}$$

In Eq. (9), y_{n+1} and A_{n+1} is the additional observations and design matrix constructed by the coordinates and intensity values of the new point (the n+1 th point) expressed as

$$y_{n+1} \equiv \begin{bmatrix} y_{I,n+1} \\ y_{II,n+1} \end{bmatrix}, A_{n+1} \equiv \begin{bmatrix} A_{I,n+1} & 0 \\ 0 & A_{II,n+1} \end{bmatrix}, \tag{12}$$

$$y_{I,n+1} = z_{n+1}, \quad A_{I,n+1} = \begin{bmatrix} x_{n+1} & y_{n+1} & 1 \end{bmatrix},$$
$$y_{II,n+1} = \begin{bmatrix} R_{n+1} \\ G_{n+1} \\ B_{n+1} \end{bmatrix}, \quad A_{II,n+1} = \begin{bmatrix} 1 & 0 & 0 \\ 0 & 1 & 0 \\ 0 & 0 & 1 \end{bmatrix}. \tag{13}$$

The test statistic T for the statistical test is then expressed as

$$T = (A_{n+1}\hat{\xi}_{(n)} - z_{n+1})^T (I_4 + A_{n+1}Q\{\hat{\xi}_{(n)}\}A_{n+1}^T)^{-1}(A_{n+1}\hat{\xi}_{(n)} - z_{n+1}) / \hat{\sigma}_{0,(n)}^2 \tag{14}$$

where $Q\{\hat{\xi}_{(n)}\}$ the cofactor matrix of the current estimate of the parameters, $\hat{\sigma}_{0,(n)}^2$ the current estimate of the variance component, and I_4 is the 4x4 identity matrix. This test statistic follows F-distribution with the degrees of freedom (4, $4n-6$) under H_0 by assuming that all the errors of the coordinates of the points and values of pixels are independent and identically normally distributed. If this test statistic is smaller than the critical value $F_a(4, 4n-6)$ of the significance level a, the null hypothesis is accepted. The tested point is then included to the patch and the estimates are updated using the sequential least square estimation summarized as

$$\hat{\xi}_{(n+1)} = \hat{\xi}_{(n)} + Q\{\hat{\xi}_{(n)}\}A_{n+1}^T(I_4 + A_{n+1}Q\{\hat{\xi}_{(n)}\}A_{n+1}^T)^{-1}(y_{n+1} - A_{n+1}\hat{\xi}_{(n)})$$
$$Q\{\hat{\xi}_{(n+1)}\} = Q\{\hat{\xi}_{(n)}\} - Q\{\hat{\xi}_{(n)}\}A_{n+1}^T(I_4 + A_{n+1}Q\{\hat{\xi}_{(n)}\}A_{n+1}^T)^{-1}A_{n+1}Q\{\hat{\xi}_{(n)}\}$$
$$\hat{\sigma}_{0,(n+1)}^2 = \frac{4n-6}{4n-2} \cdot \hat{\sigma}_{0,(n)}^2 + \frac{(A_{n+1}\hat{\xi}_{(n)} - y_{n+1})^T(I_4 + A_{n+1}Q\{\hat{\xi}_{(n)}\}A_{n+1}^T)^{-1}(A_{n+1}\hat{\xi}_{(n)} - y_{n+1})}{4n-2}. \tag{15}$$

3. Experimental Results

3.1 Test Data

The proposed method has been applied to five different data sets. Each data set includes the LIDAR data and the aerial images, which were simultaneously acquired

by a LIDAR system and a medium-format digital camera mounted to the same airplane. Their main properties are summarized in Table 1.

These data sets cover an urban area in Masan, Korea. This area includes mainly large buildings of various shapes on the almost flat terrain as shown in Fig. 2. Set A mainly includes mainly planar roof surfaces of various slopes which are very adjacent each other. Set B includes buildings looking similar to those in Set A but their roof surfaces are quite near to each other, retaining slight height differences. Hence, the successful segmentation of these individual surfaces is thought to be significantly difficult. This is the reason why we selected this set to evaluate the proposed method. Set C includes buildings of common shapes with different sizes. Each of them mainly has a large flat roof on which small objects locate.

3.2 Evaluation Procedures

To validate the proposed segmentation method, we need to evaluate quantitatively the segmentation results from its application to the test data. This quantitative evaluation is based on the comparison of the segmentation results with a reference model assumed to be true. Hence, in this study, we created this reference model by manually digitizing an ortho-rectified aerial image over the test area, as shown in Fig. 3. This manual digitization was applied to the large surfaces mainly corresponding to the roofs of large buildings, which can be distinctly recognizable from the visual inspection.

During the evaluation process, we compare a set of automatically segmented patches with its corresponding reference sets of manually segmented patches. During this comparison processes, we try to find the correspondence between the patches of the automatically segmented set and those of the reference set by computing the overlapping area of each patch from a set with each patch from the other set. Based on the correspondence, we assign five different classes indicating the correctness of segmentation, which are "correct", "over-segmented", "under-segmented", "noises", and "not segmented". Each of these classes is explained in more detail as follows:

Table 1. Properties of Data Sets

ID	LIDAR			Images
	No. points	Area [m^2]	Point density [points/m^2]	Ground resolution [cm]
A	16561	7356.41	2.25	20
B	10207	5776.70	1.77	
C	19862	9176.16	2.16	

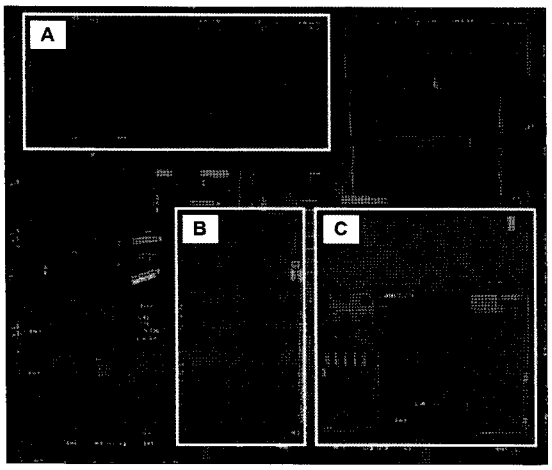

Fig. 2. Data coverage over the aerial image

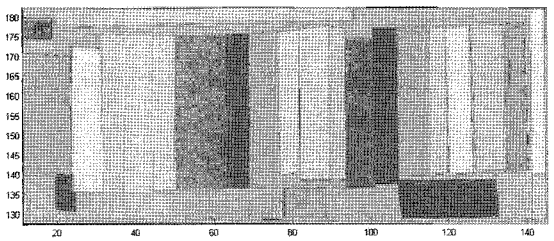

(a)

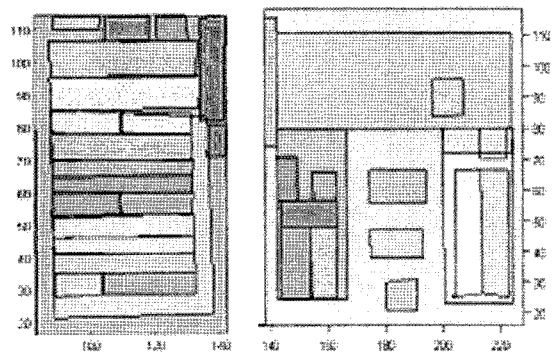

(b) (c)

Fig. 3. A Manually Segmented Reference Model

(A) Correct (C): if a patch from the automatically segmented set is almost identical to its corresponding patch from the reference set, "correct" is assigned. In this case, the shapes of two patches are similar and their overlapping area is more than 80% of the area of each patch.

(B) Over-segmentation (OS): if more than two patches from the automatically segmented set correspond to only a patch from the reference set, "over-segmentation" is assigned. In this case, a surface patch in reality is divided into more than two patches from the segmentation process. This is usually caused when the initial patch for the region growing is not enough large to retain the average properties of a patch in reality or the threshold for the region growing is too small. In general, if we set a lower value to the significance level in the statistical test to determine if a point is consistent with a currently growing patch, we can decrease the occurrence of type I error of the statistical test but face the over-segmentation problem.

(C) Under-segmentation (US): if a patch from the automatically segmented set corresponds to more than two patches from the reference set, "under-segmentation" is assigned. In this case, more than two patches in reality are merged into a patch from the segmentation process. This is usually caused when the initial patch for the region growing happen to overlap more than two patches in reality or the threshold for the region growing is too large. In general, if we set a higher value to the significance level in the statistical test, we can decrease the occurrence of type II error of the statistical test but face the under-segmentation problem. In addition, if the distance between two different patches of similar properties is not enough large in comparison with the average distance between points, they may be segmented into a single patch rather than two separate patches. An example of this kind is shown in Fig. 4.

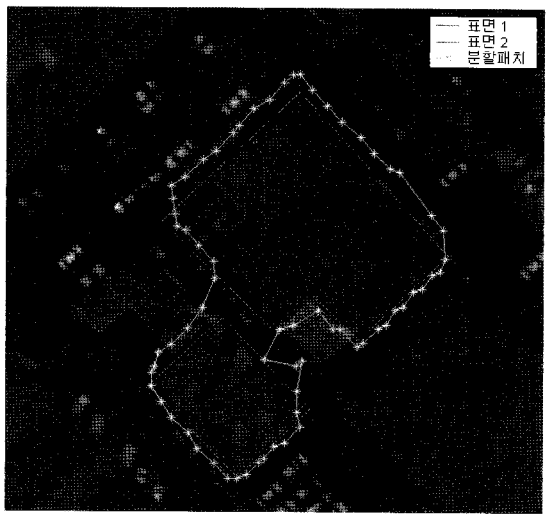

Fig. 4. An Example of Under-segmentation

(D) Noise (N): if a patch from the automatically segmented set corresponds to none of patches from the reference set, "noise" is assigned. In this case, the automatically segmented patch is decided not to exist in reality. This can be usually caused if erroneous points (like outliers) were not eliminated during the preprocessing process and remain aggregated in a local area or a patch existing in reality is omitted during the manual segmentation process.

(E) Not segmented (NS): if a patch from the reference set corresponds to none of patches from the automatically segmented set, "not segmented" is assigned. In this case, the automatic segmentation process fails to extract a patch existing in reality.

3.3 Segmentation Results and Evaluation

The proposed segmentation method was applied to three data sets described before. During this experiment, the significance level in the statistical test for region growing is set to 0.5%. The segmentation results from Set A are shown in Fig. 5, where (a) visualizes the points grouped into each patch and (b) does the boundary of each patch. The boundary is computed using the alpha-shape algorithm (Edelsbrunner et. al., 1983). We had attempted to assign different colors to different patches but we used only six different colors since we cannot visually recognize more than six colors. Some different patches may have the same colors, hence. In the similar way, the segmentation results from Set B and Set B are shown in Fig. 6 and 7, respectively.

All the segmentation results look visually reasonable. All the main planar surfaces locating on the large buildings are successfully segmented. The results were further quantitatively evaluated according to the criteria descri-

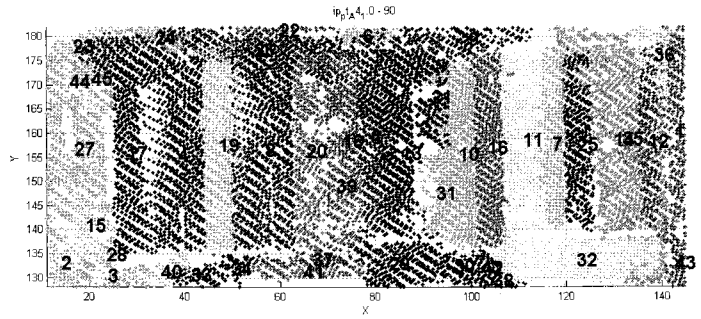

(a)

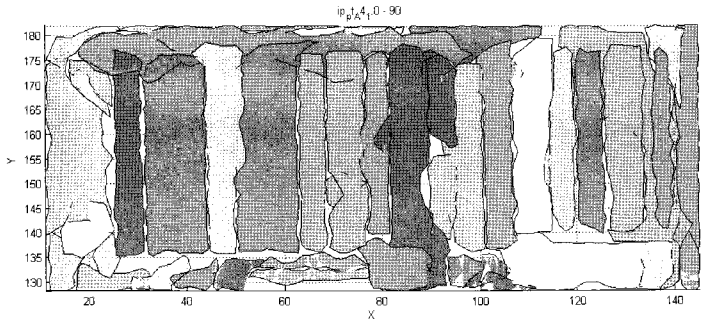

(b)

Fig. 5. Segmentation Results of Set A

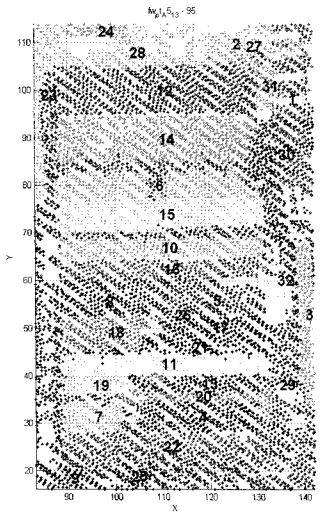

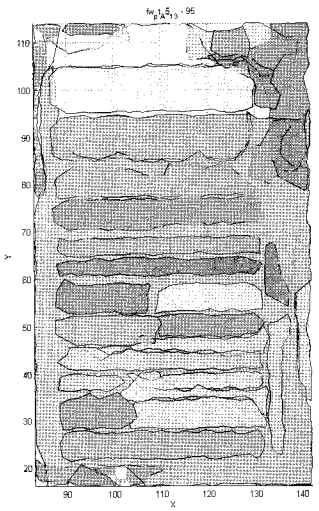

(a) (b)

Fig. 6. Segmentation Results of Set B

bed in the previous section. This evaluation results are summarized in Table 2. In overall, about 76% area of total area of the entire sets are correctly segmented into 52 patches. Fifteen patches (about 11% of total area) existing in reality are over-segmented and two patches are under-segmented. Hence, it can be seen that the proposed segmentation method tends to divide a patch in reality into more than two patches during the seg-

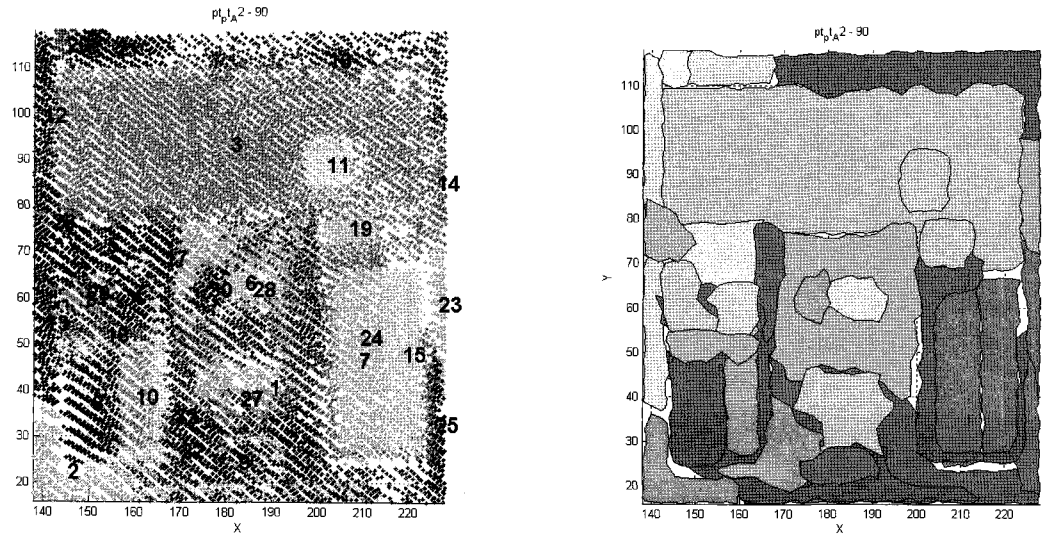

Fig. 7. Segmentation Results of Set C

Table 2. Quantitative Evaluation Results

		C	OS	US	N	NS	Total
Set A	No. patches	23	3	1	10	0	37
	Area [m^2]	6106.03	766.63	507.4	1036.15	0	8416.21
	Area Ratio [%]	72.6	9.1	6.0	12.3	0	100
Set B	No. patches	14	6	1	4	0	25
	Area [m^2]	2633.21	540.7	233.95	416.65	0	3824.51
	Area Ratio [%]	68.9	14.1	6.1	10.9	0	100
Set C	No. patches	15	6	0	4	0	25
	Area [m^2]	6103.08	798.4	0	476	0	7377.48
	Area Ratio [%]	82.7	10.8	0	6.5	0	100
Total	No. patches	52	15	2	18	0	87
	Area [m^2]	14842.32	2105.73	741.35	1928.8	0	19618.2
	Area Ratio [%]	75.7	10.7	3.8	9.8	0	100

mentation process in some cases. This over-segmentation problem can be mitigated by incorporating a post-processing process to merge recursively two different adjacent patches with similar properties into a patch. In other hand, many noisy small patches are generated from the proposed segmentation process. Some of these are the patches actually existing in reality that we could not clearly recognize during the digitization process for the generation of the reference set. The others can be eliminated by checking if their properties are reasonable in the real world in terms of the size, roughness, and shape.

4. Conclusion

In this study, we proposed a region-based segmentation approach to generate a set of patches representing the terrain by grouping the LIDAR points based on the coordinates of the points and the corresponding image intensity values. This approach mainly consists of seed patch generation and iterative patch growing. A statistical test to examine the consistency between a new point and a currently growing patch is presented with mathematical derivation.

From the experimental results from its application to urban data, the proposed method produces correct segmentation in 76% of the test area comparing to the reference data acquired by manual segmentation. About 11% area is over-segmented, indicating that a post-processing process to merge adjacent patches with similar properties is required. In about 10% area, the noisy patches are generated. This is mainly because the manual segmentation can often ignores small patches. Relatively, the small area (4%) is under-segmented. This low ratio can be achieved since both LIDAR data and image are used. Under-segmentation has been reported as a significant problem particularly in a dense urban area if only LIDAR data are used.

If the over-segmentation problem is mitigated by incorporating a post process to merge adjacent patches with similar properties, we can effectively utilize the proposed segmentation method as a reliable intermediate process toward automatic extraction of 3D model of the real world.

Acknowledgement

We would like to express our great appreciation to the researchers in Hanjin Information Systems & Telecommuncation Co. Ltd. for their providing the LIDAR data and images used for testing the proposed method.

References

Brenner, C. (2003). "Building reconstruction from laser scanning and images." Proc. ITC Workshop on Data Quality in Earth Observation Techniques, Enschede, The Netherlands.

Edelsbrunner, H., Kirkpatrick, D.G. and Seidel, R. (1983). "On the shape of a set of points in the plane." IEEE Transactions on Information Theory, Vol. 29, No. 4, pp. 551-559.

Kim, S.J. (2006). 3D Geometric Road Modeling from LIDAR Data and Digital Map, MSc. Thesis, The University of Seoul, Seoul, Korea.

Lee, I. (2002). Perceptual Organization of Surfaces, Ph.D. Dissertation, Dept. of Civil and Environmental Engineering and Geodetic Science, The Ohio State University, Columbus, OH, USA.

Lee, I. (2006a). "Segmentation of Airborne LIDAR Data: From Points to Patches." Korean Journal of Geomatics, Vol. 25, No. 4, pp. 111-121.

Lee, I. (2006b). "Automatic Extraction of Ground Points from LIDAR data." Korean Journal of Remote Sensing, Vol. 22, No. 4, pp. 265-274.

Lee, I. and Schenk, T. (2001a). "Autonomous extraction of planar surfaces from airborne laser scanning data." ASPRS Annual Conference, American Society for Photogrammetry and Remote Sensing, St. Louis, MO, USA.

Lee, I. and Schenk, T. (2001b). "3D Perceptual Organization of Laser Altimetry Data." Proc. ISPRS WG III/3-6 Workshop on "Land surface mapping and characterization using laser altimetry", International Archives of Photogrammetry and Remote Sensing, International Society for Photogrammetry and Remote Sensing, Annapolis, MD, USA, Vol. 34, Part 3/W4, pp. 57-65.

Lee, I. and Schenk, T. (2002). "Perceptual organization of 3D surface points." Proc. ISPRS Commission III Symposium on "Photogrammetric Computer Vision", International Archives of Photogrammetry and Remote Sensing, International Society for Photogrammetry and Remote Sensing, Graz, Austria. Vol. 34, Part 3A, pp. 193-198.

Lee, I., Kim, S.J. and Choi, Y. (2005). "Surface-based Geometric Registration of Aerial Images and LIDAR Data." Korean Journal of Geomatics, Vol. 5, No. 1, pp. 35-42.

Lodha S. K., Kumar, K. and Kuma, A. (2005). "Semi-automatic roof reconstruction from aerial LIDAR data using K-means with refined seeding." ASPRS Conference, American Society for Photogrammetry and Remote Sensing, Baltimore, Maryland.

Moon J., Lee, I., Kim, S. and Kim, K. (2005). "Outlier Detection from LIDAR Data based on the Point Density." Korean Society Civil Engineering Journal, Vol. 25, No. 6D, pp. 891-897.

Park, J., Lee, I., Choi, Y. and Lee, Y.J. (2006). "Automatic Extraction of Large Complex Buildings using LIDAR Data and Digital Maps." Proc. ISPRS Commission III Symposium on "Photogrammetric Computer Vision", International Archives of Photogrammetry and Remote Sensing, International Society for Photogrammetry and Remote Sensing, Bonn, Germany, Vol. 36, Part 3, pp. 148-154.

Rottensteiner, F and Briese, C. (2003). "Automatic Generation of Building Models from LIDAR Data and the Integration of aerial image." Proc. ISPRS WGIII/3 Workshop on "3-D reconstruction from airborne laserscanner and InSAR data", International Archives of Photogrammetry and Remote Sensing, International Society for Photogrammetry and Remote Sensing, Dresden, Germany, Vol. 34, Part 3/W13.

Schenk, T., and Csatho, B. (2002). "Fusion of LIDAR data and aerial imagery for a more complete surface description." Proc. ISPRS Commission III Symposium on "Photogrammetric Computer Vision", International Archives of Photogrammetry and Remote Sensing, International Society for Photogrammetry and Remote Sensing, Vol. 34, Part 3A, pp. 310-317.

(접수일 2007. 12. 14, 심사일 2007. 12. 17, 심사완료일 2007. 12. 19)